Spatially resolved proteomics via tissue expansion
基于组织膨胀的空间蛋白质组学

李璐 Lu Li

2022.11.29

西湖大學
WESTLAKE UNIVERSITY

The importance of spatial proteomics in medicine

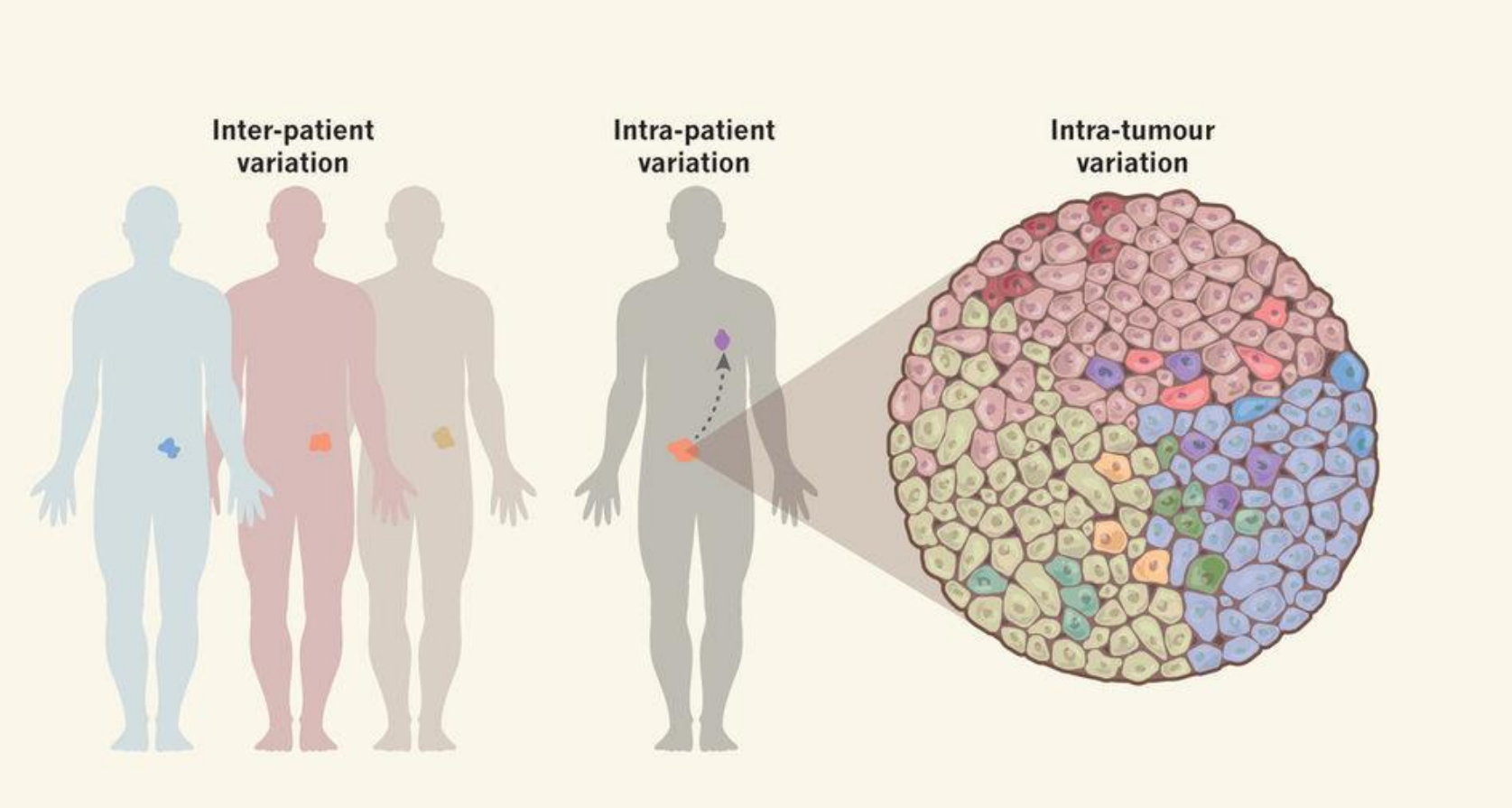

Nature Reviews Cancer volume 19 (2019)

Microsampling techniques for spatial proteomics

laser capture microdissection (LCM)

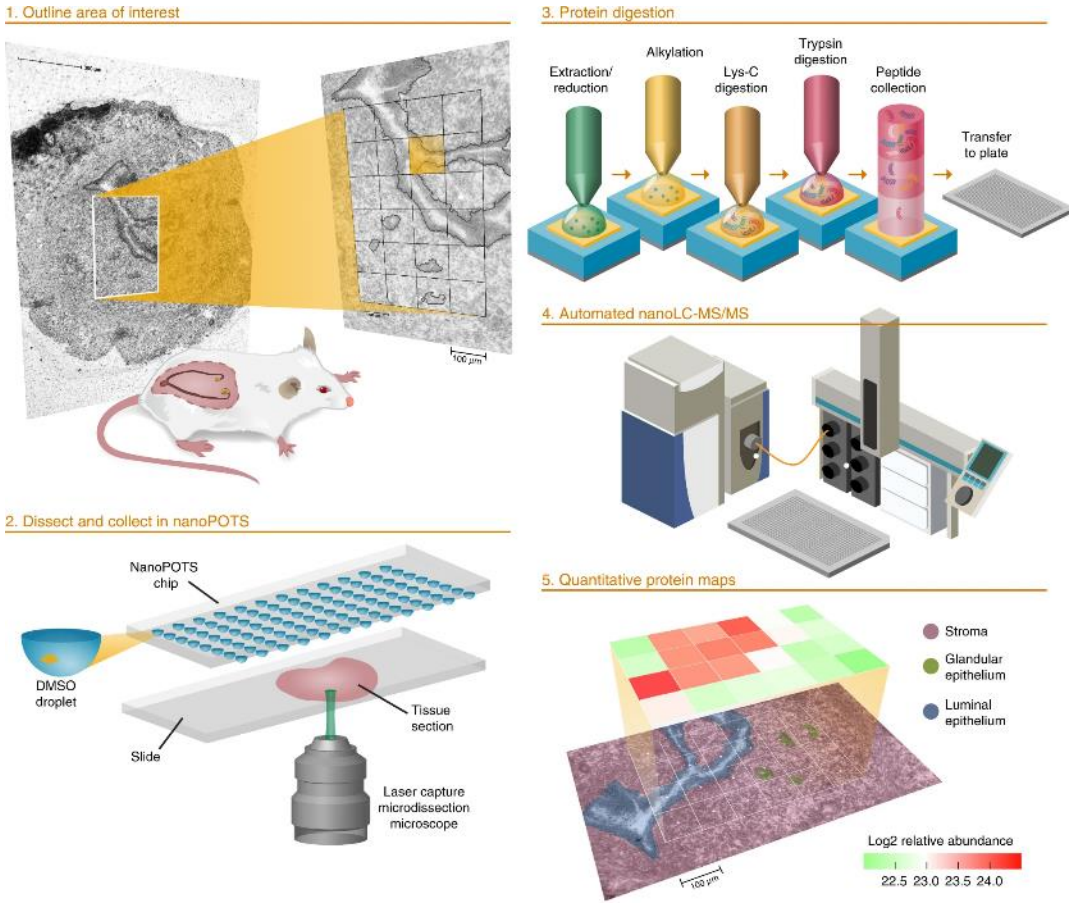

matrix-assisted laser desorption/ionization (MALDI)

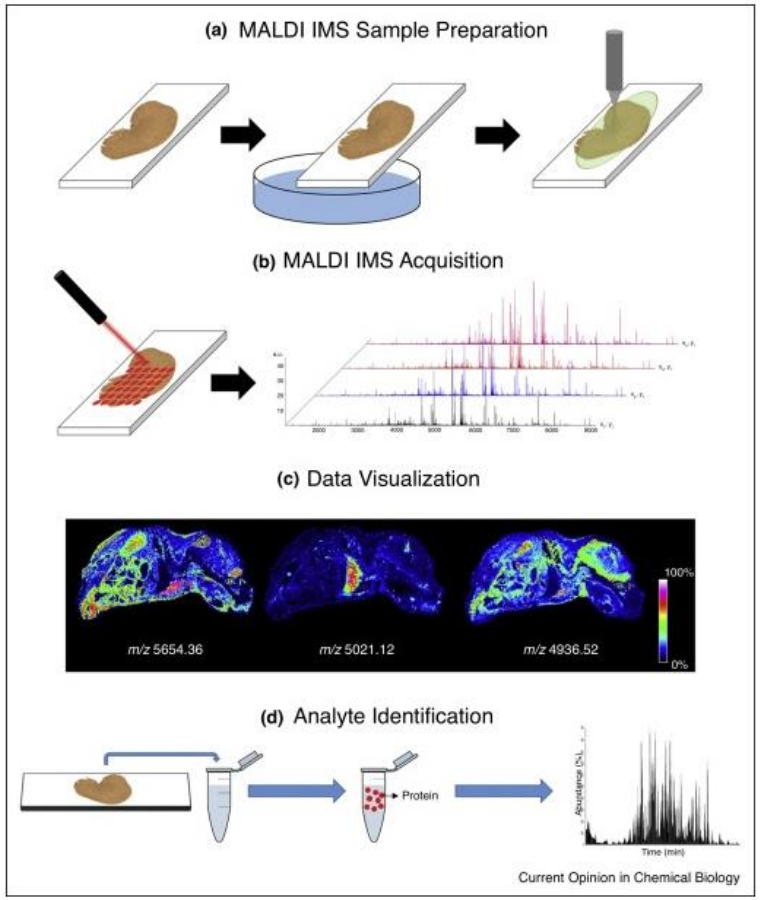

Nat Commun. 2020 Jan 7;11(1):8.
Curr Opin Chem Biol. 2019 Feb;48:64-72.

Spatial proteomics

OPTICAL IMAGING

Expansion microscopy

Fei Chen,[1*] Paul W. Tillberg,[2*] Edward S. Boyden[1,3,4,5,6†]

In optical microscopy, fine structural details are resolved by using refraction to magnify images of a specimen. We discovered that by synthesizing a swellable polymer network within a specimen, it can be physically expanded, resulting in physical magnification. By covalently anchoring specific labels located within the specimen directly to the polymer network, labels spaced closer than the optical diffraction limit can be isotropically separated and optically resolved, a process we call expansion microscopy (ExM). Thus, this process can be used to perform scalable superresolution microscopy with diffraction-limited microscopes. We demonstrate ExM with apparent ~70-nanometer lateral resolution in both cultured cells and brain tissue, performing three-color superresolution imaging of ~10^7 cubic micrometers of the mouse hippocampus with a conventional confocal microscope.

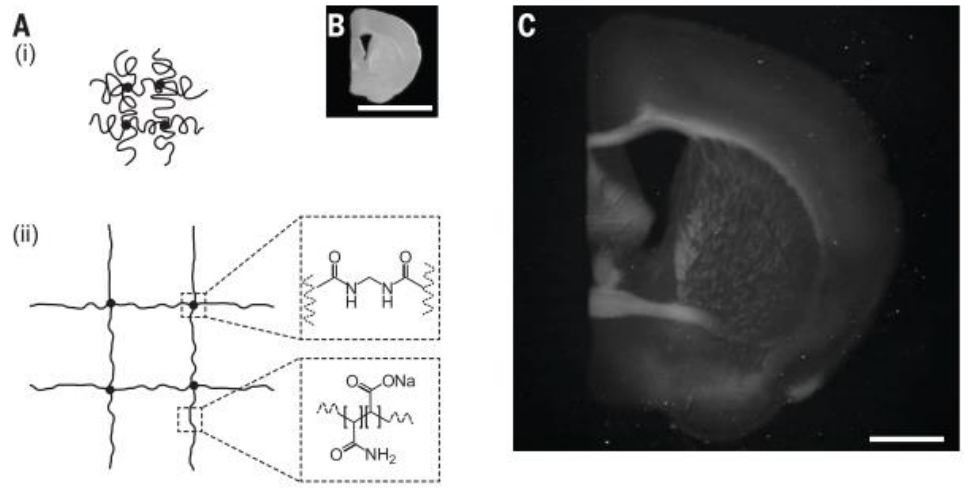

Science (2015)

TECHNOLOGY FEATURE

TECHNOLOGY TO WATCH IN 2018

Thought leaders reveal the technologies and topics likely to transform life-science research in the year ahead.

The Internet of Things has transformed many aspects of our lives and is now, along with other breakout technologies, poised to transform life-science research.

SWATH/DIA

Nature (2018)

nature methods ARTICLES https://doi.org/10.1038/s41592-020-00998-0

diaPASEF: parallel accumulation–serial fragmentation combined with data-independent acquisition

Florian Meier[1,2], Andreas-David Brunner[1], Max Frank[3], Annie Ha[3], Isabell Bludau[1], Eugenia Voytik[1], Stephanie Kaspar-Schoenefeld[4], Markus Lubeck[4], Oliver Raether[4], Nicolai Bache[5], Ruedi Aebersold[4,7], Ben C. Collins[4,8] ✉, Hannes L. Röst[3] ✉ and Matthias Mann[1,9] ✉

4D-Proteomics

Nature Methods (2020)

ProteomEx

ProteomEx = Proteomics + Expansion

We describe a spatially resolved proteomics method based on the combination of tissue expansion with mass spectrometry-based proteomics. ProteomEx enables quantitative profiling of the spatial variability of the proteome in mammalian tissues at ~160 μm lateral resolution, equivalent to the tissue volume of 0.61 nL, using manual microsampling without the need for custom or special equipment.

ProteomEx workflow development and optimization

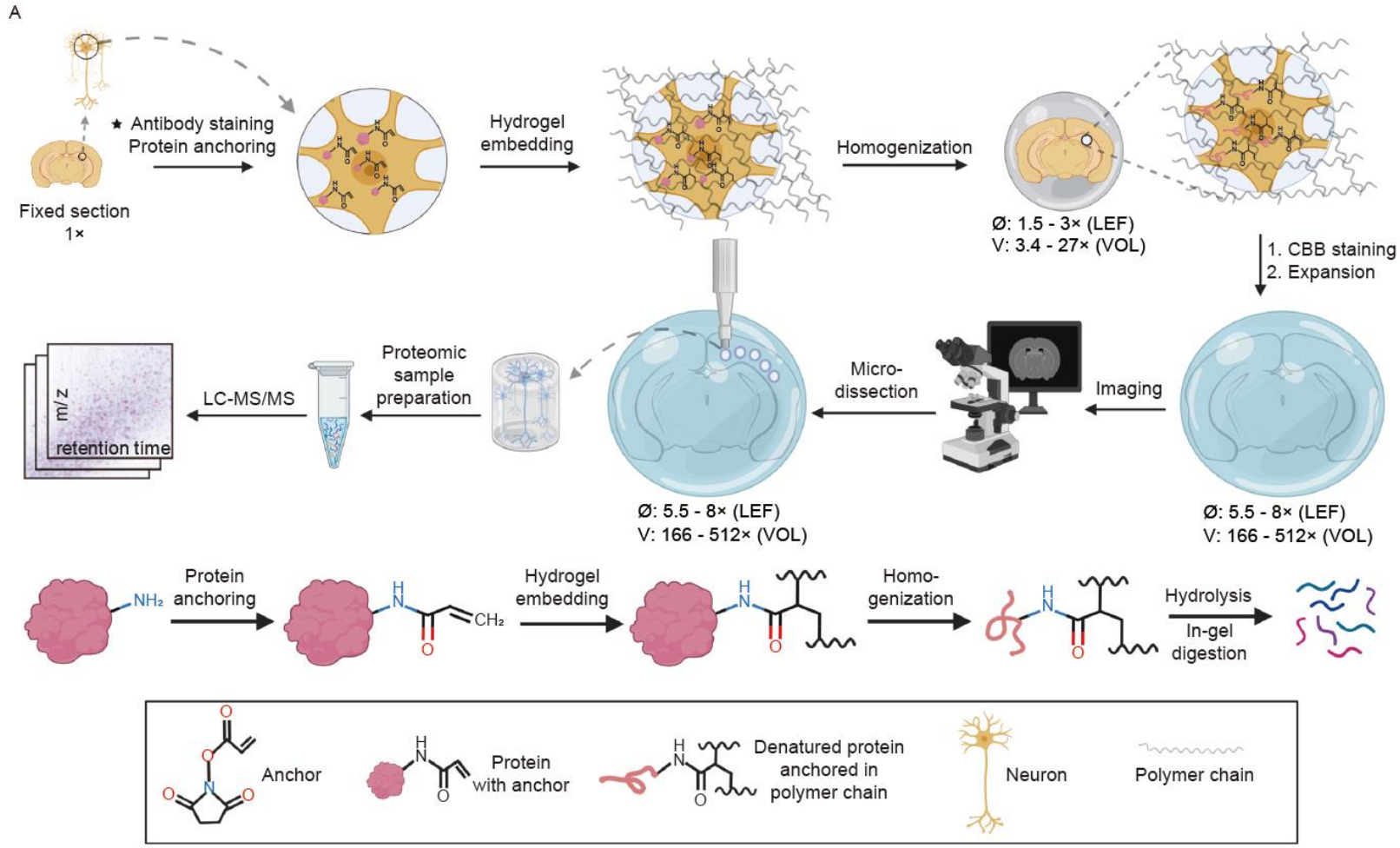

i) an optimized hydrogel with enhanced expansion factor and mechanical stability; ii) reversible protein anchoring to polymer network; iii) isotropic expansion of sample; iv) sample staining; v) sample microdissection; vi) in-gel digestion and peptide extraction

ProteomEx workflow development and optimization

B

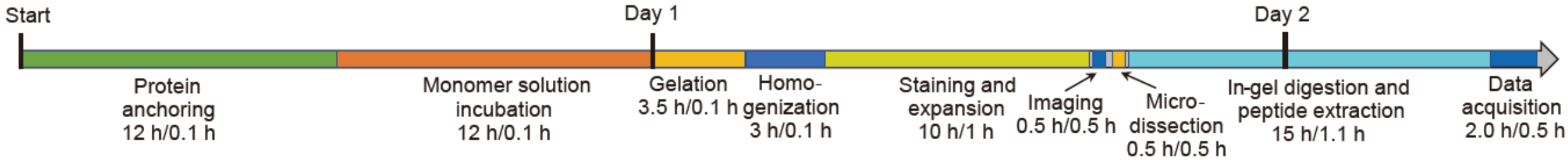

Imaged by bright field microscope

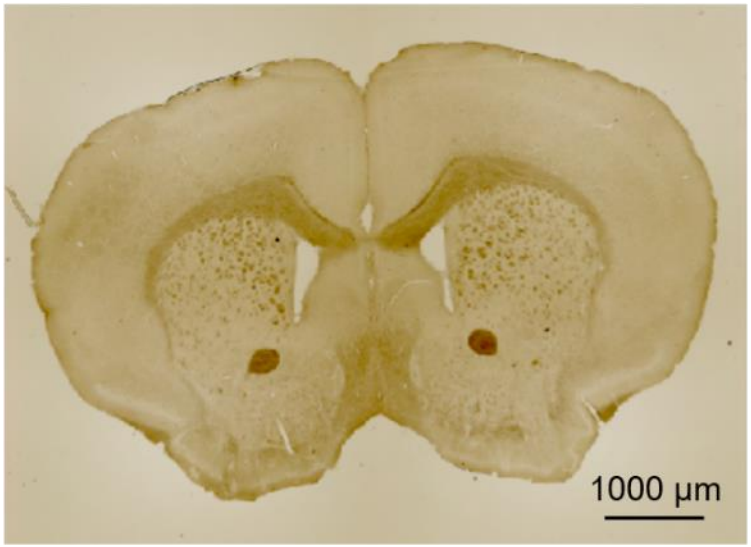

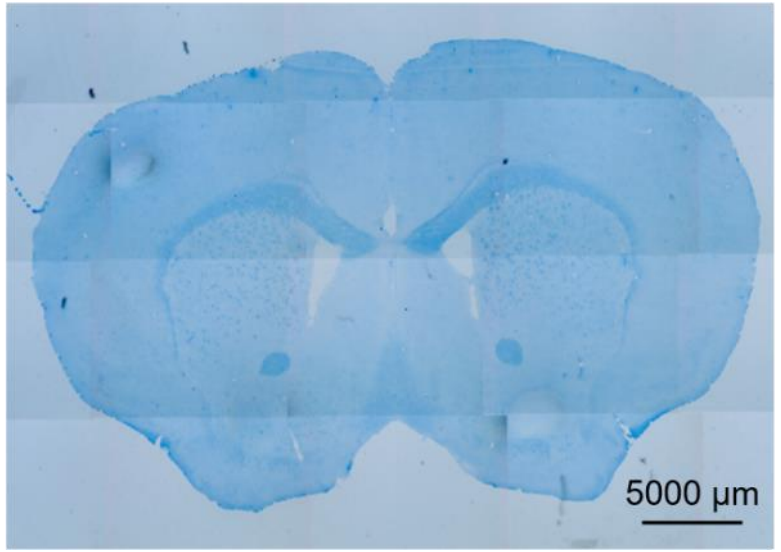

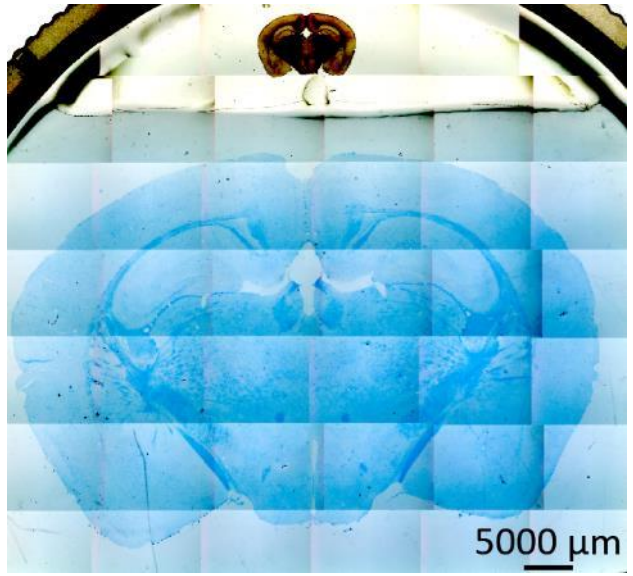

While it takes about 58 hours to process fixed samples, the required hands-on time is only 5 h, *i.e.*, less than 10% of total duration.

ProteomEx validation and characterization

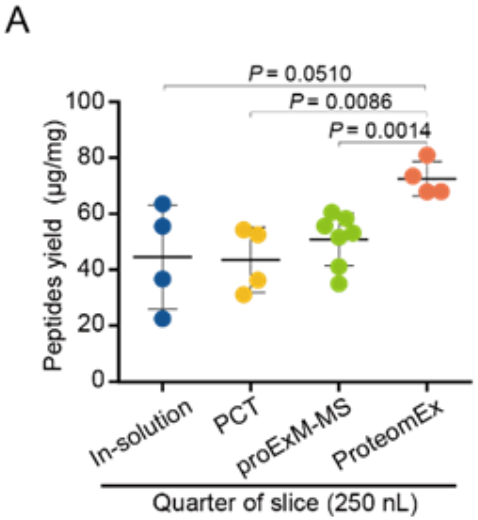

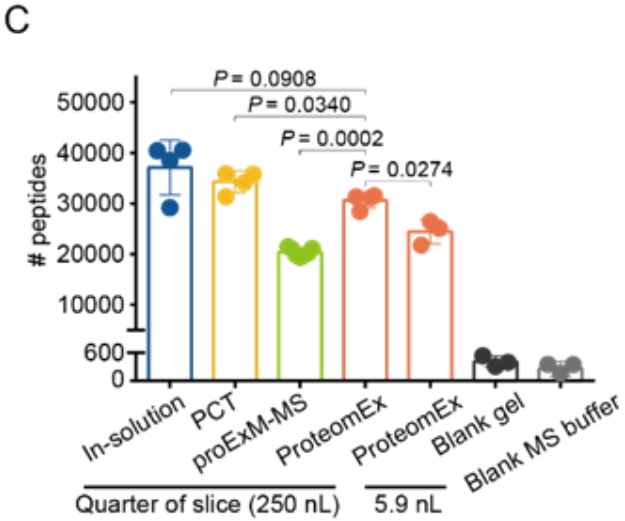

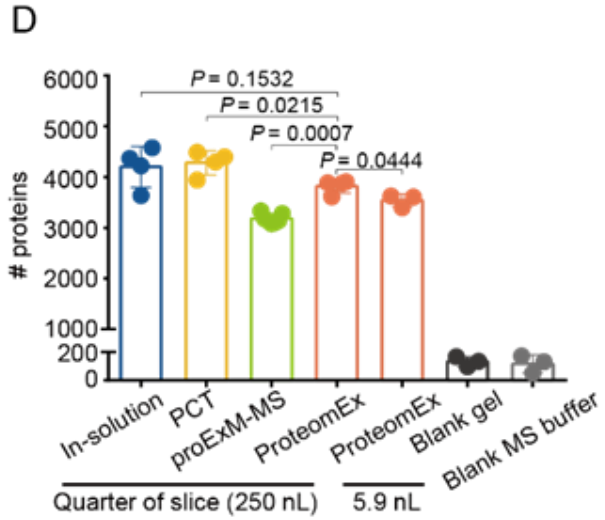

# Pep	#Prot
37,173	4199
34,304	4278
20,413	3181
30,630	3818

# Pep	#Prot
24,437	3541
416	132
260	116

More peptide yield (1.4-1.7 fold)

Comparable counts of identified proteins

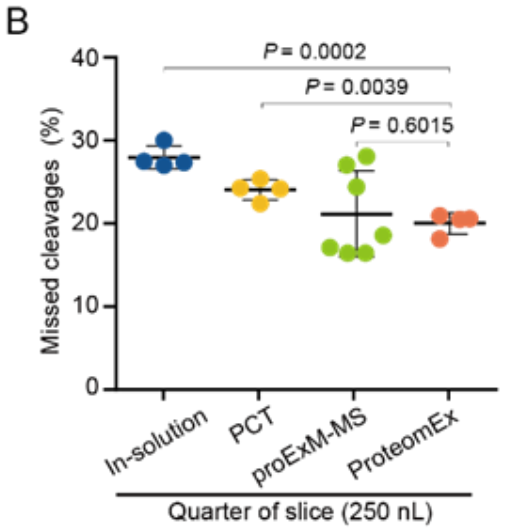

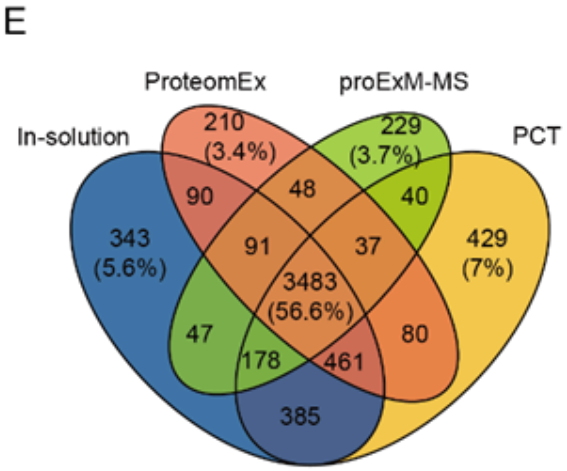

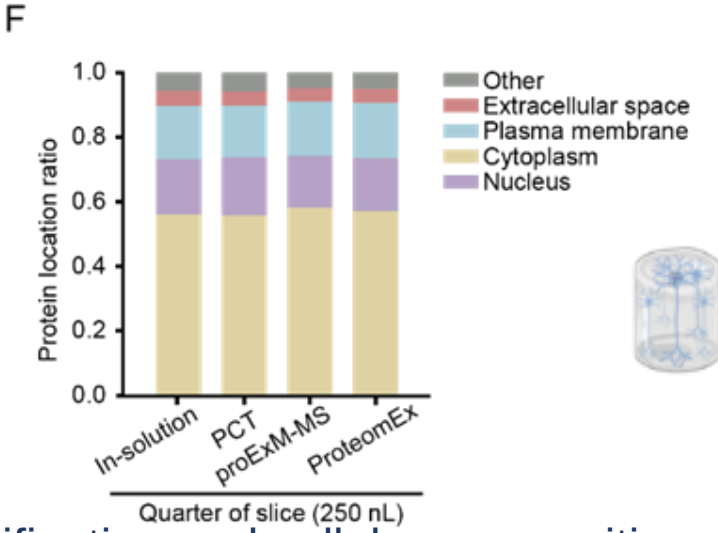

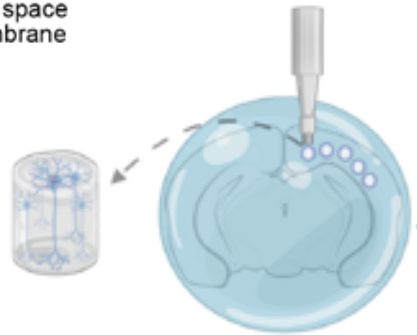

Less missed cleavages (20.4±1.0%)

Similar protein identification and cellular composition

Explored the volume-dependent limit of tissue microsampling using ProteomEx approach

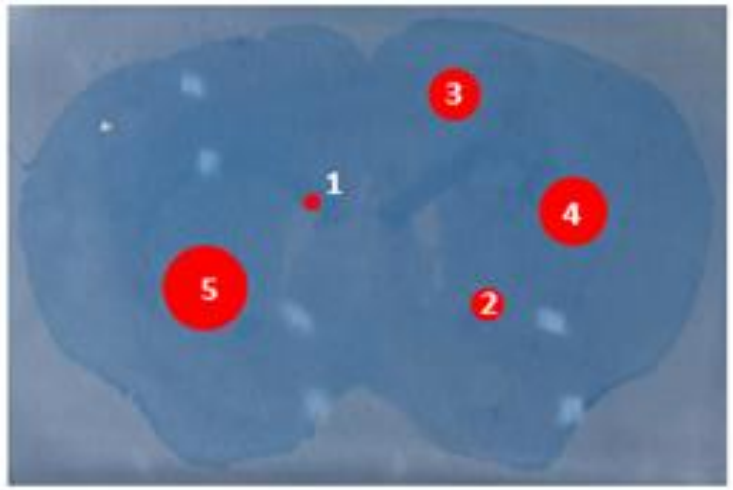

G

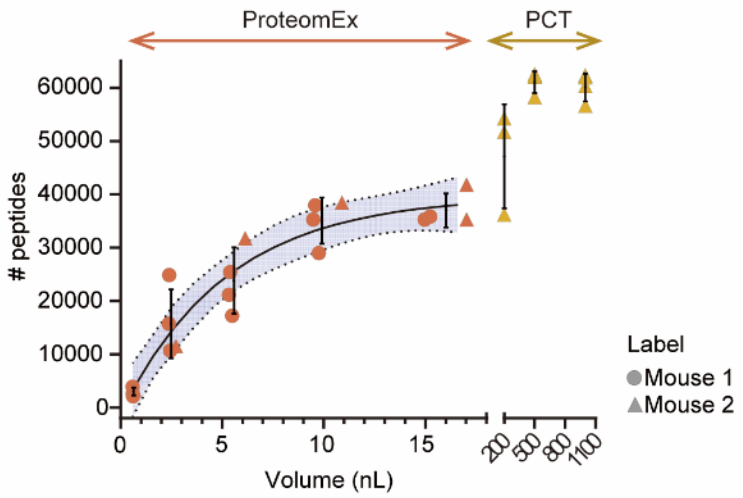

H

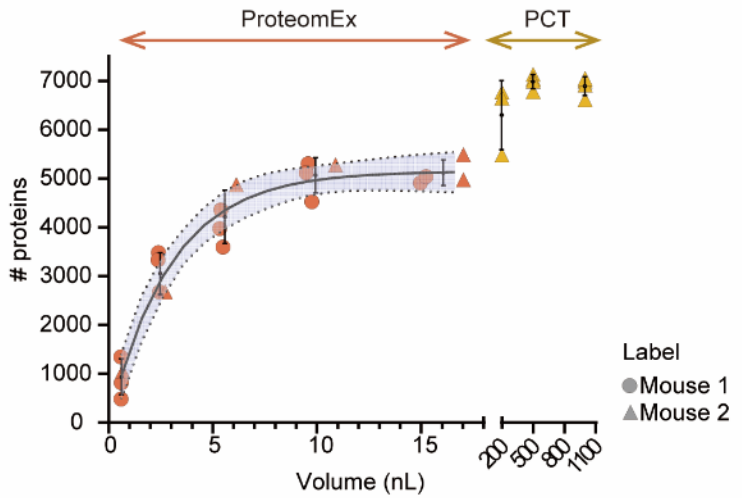

Biopsy punches	1 mm	2 mm	3 mm	4 mm	5 mm
Lateral resolution	160 µm	320 µm	480 µm	640 µm	800 µm
Tissue volume	0.6 nL	2.4 nL	5.4 nL	9.6 nL	15.0 nL
# peptides	2987	15,705	23,898	35,160	37,071
# proteins	928	3044	4203	5058	5105

To assess the applicability of ProteomEx to various mammalian tissues

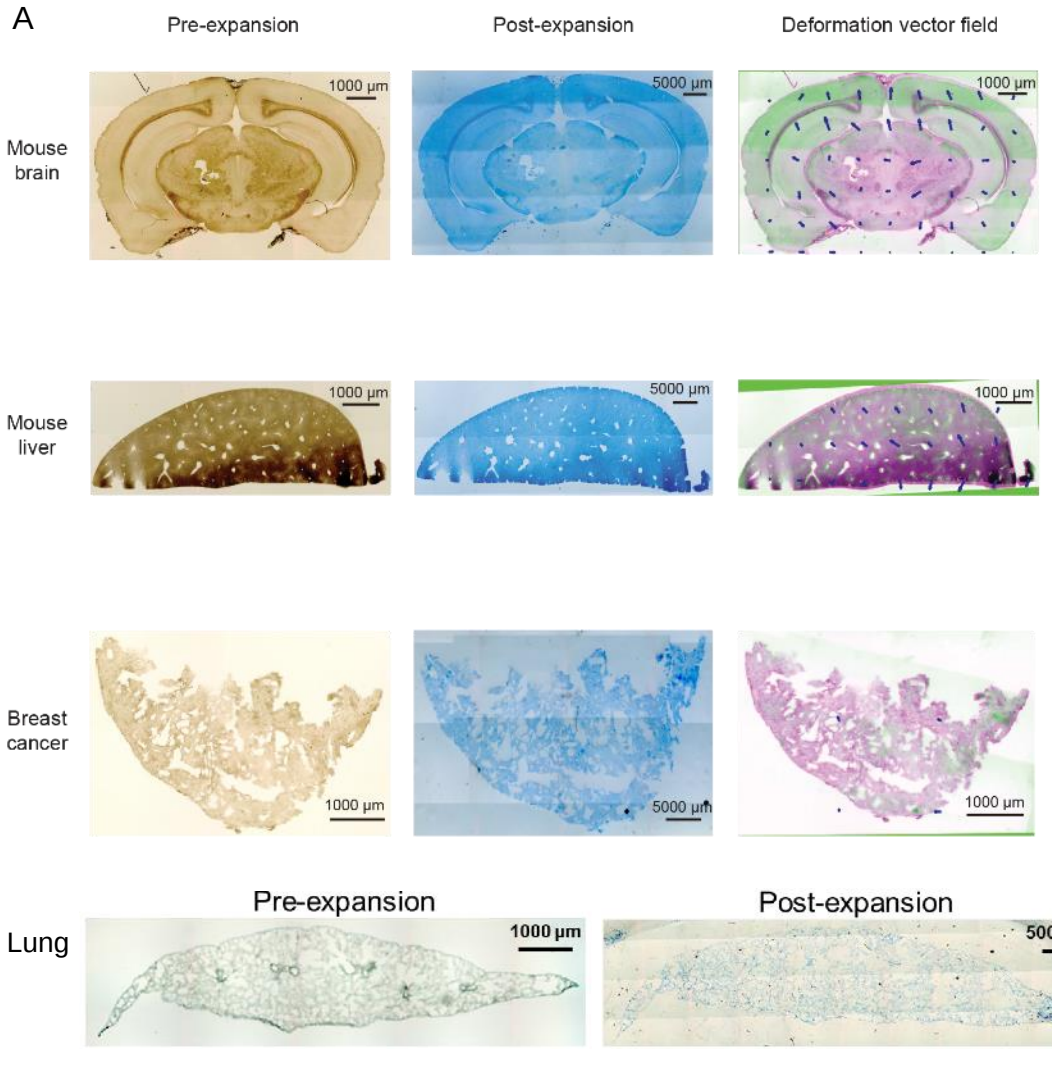

We processed ~5 nL volume of each tissue type using DDA-MS and identified 24,436/3540, 14,298/2606, 9623/2356 peptides/proteins for brain, liver, and breast cancer samples, respectively.

The root-mean-square (RMS) errors for multiple tissue types were <10%.

ProteomEx: Staining

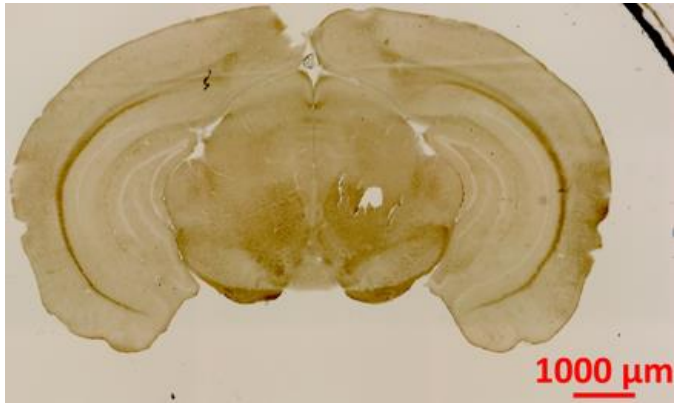

Original tissue (pre-expansion)

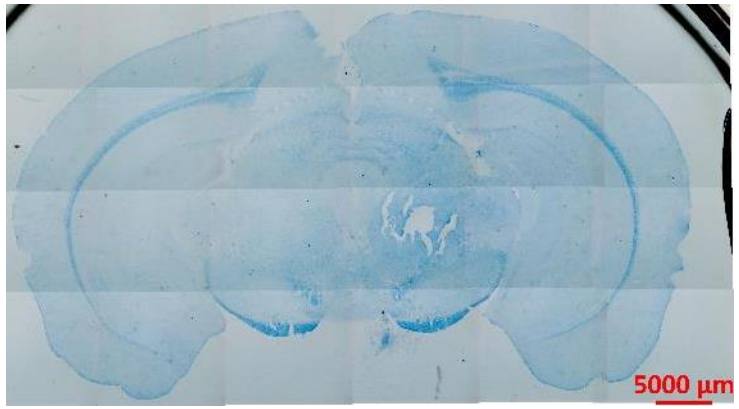

Coomassie blue staining

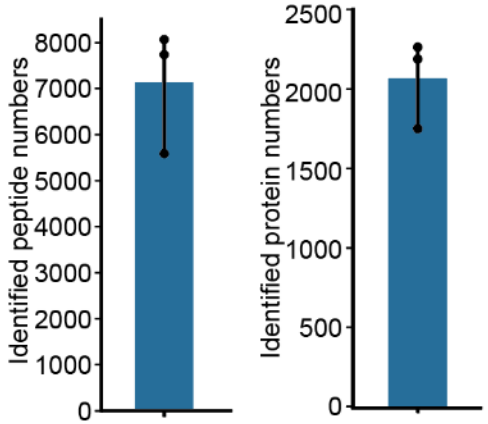

Proteomic identification

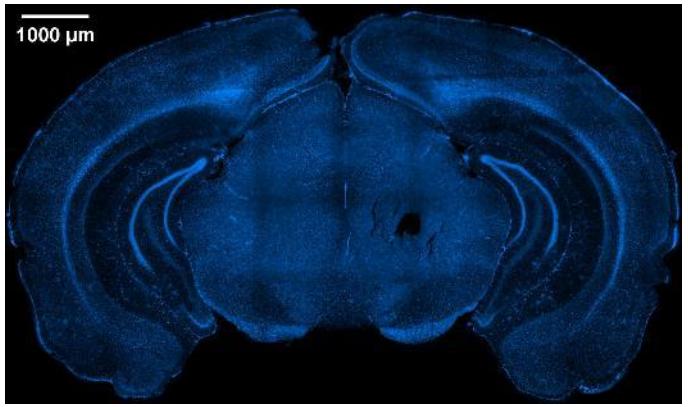

DAPI staining

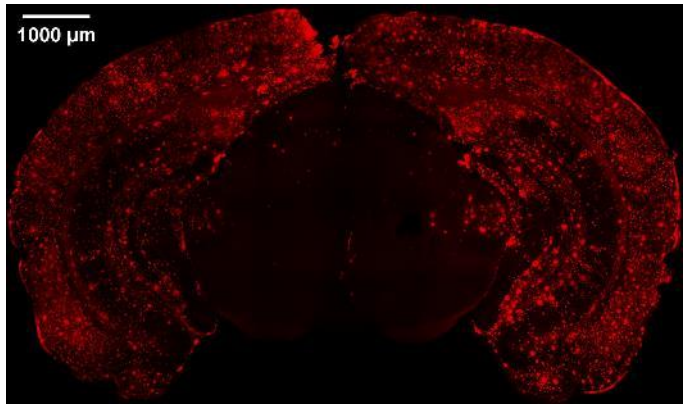

Aβ immunostaing

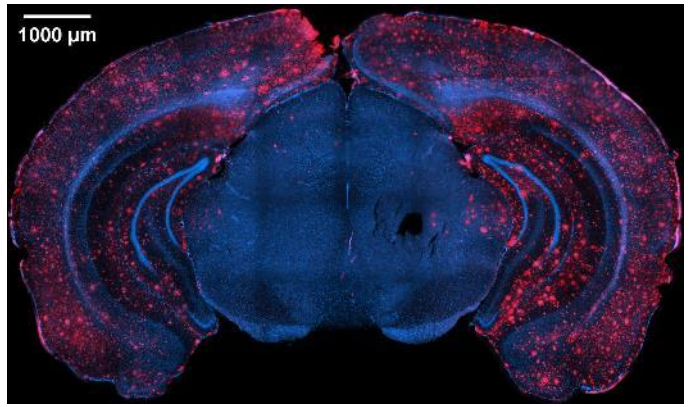

Merged

For the 2.52 nL volume of the immunostained tissue, we identified 7000 peptides corresponding to 2000 proteins for three replicates.

To explore the limits of lateral spatial resolution and tissue volume

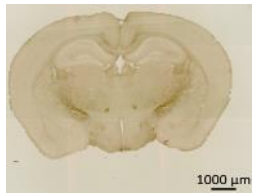

Pre-expansion

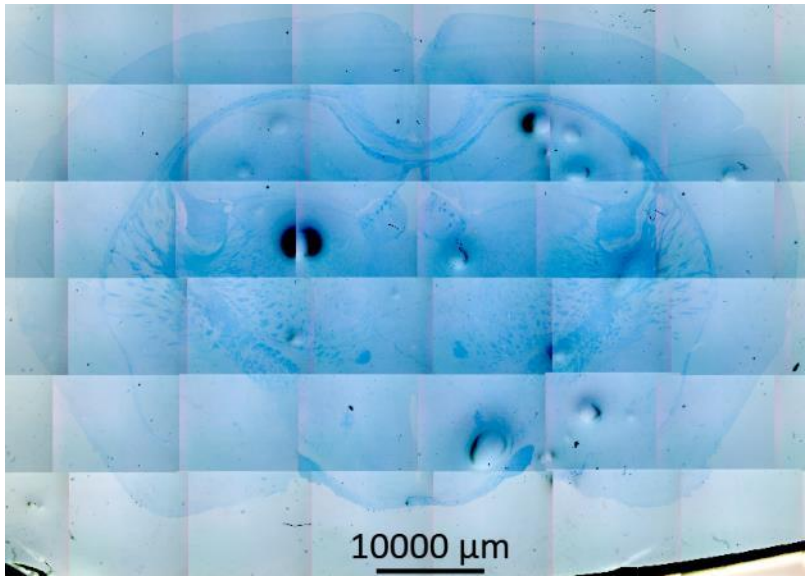

8-fold expansion

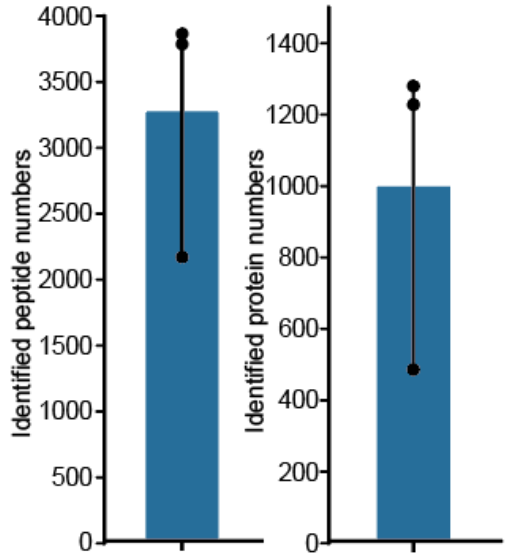

Identification of 1 mm-diameter punch gels

8-fold in linear dimension (512-fold in volume)
The pre-expansion radius of 125 μm
The pre-expansion volume of tissues was 0.37 nL, equivalent to approximately 160 cells identified and quantified more than 3000 peptides, and 1000 proteins

Proteomic profiling of normal and pathogenic brain tissue with subregion precision

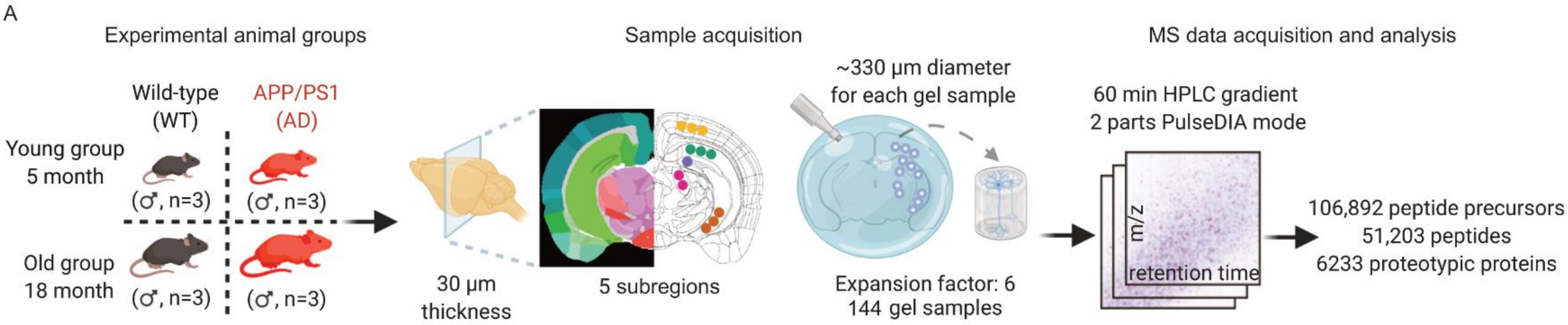

(A) Study design of proteomic analysis of the wild-type and AD mouse model representing (1) experimental animal groups (n=3 mice per group), (2) sample acquisition, (3) MS data acquisition and analysis. Brain subregions selected namely, primary visual cortex (V1, n=3 punches per slice per mouse), hippocampal field CA1 (CA1, n=3 punches per slice per mouse), hippocampal field CA3 (CA3, n=3 punches per slice from per mouse), dentate gyrus (DG, n=1 punch per slice per mouse), and medial geniculate complex (MGC, n=2 punches per slice per mouse). Created with Biorender.com.

Proteomic profiling of normal and pathogenic brain tissue with subregion precision

B

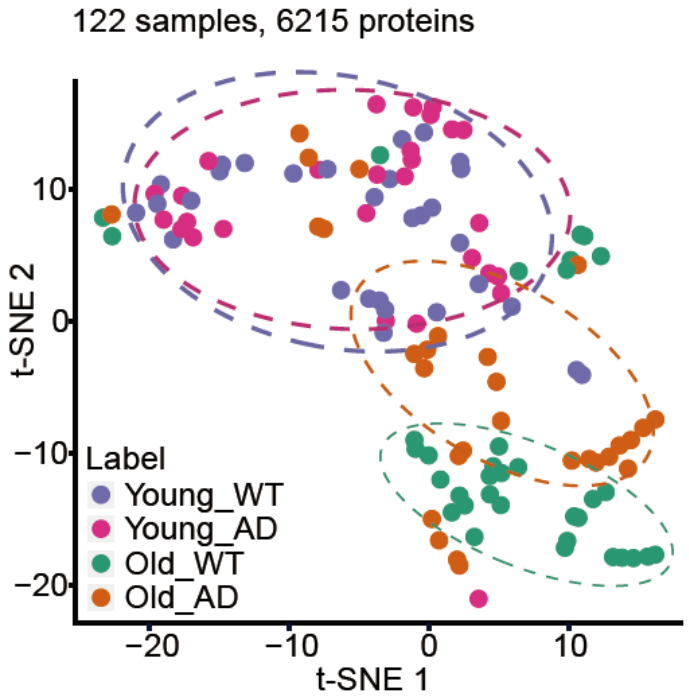

C

Age	Region	Subregion	Proteins	Down	Up	All
Young	All	-	5152	0	1	1
	Cortex	V1	4581	0	1	1
	Hippocampus	All	4870	0	2	2
		CA1	4481	0	0	0
		CA3	4165	0	0	0
		DG	3933	0	0	0
	MGC	-	3791	0	0	0
Old	All	-	6170	72	12	84
	Cortex	V1	5672	3	3	6
	Hippocampus	All	6046	66	7	73
		CA1	5576	192	6	198
		CA3	5706	18	1	19
		DG	5467	0	0	0
	MGC	-	5203	1	0	1

D

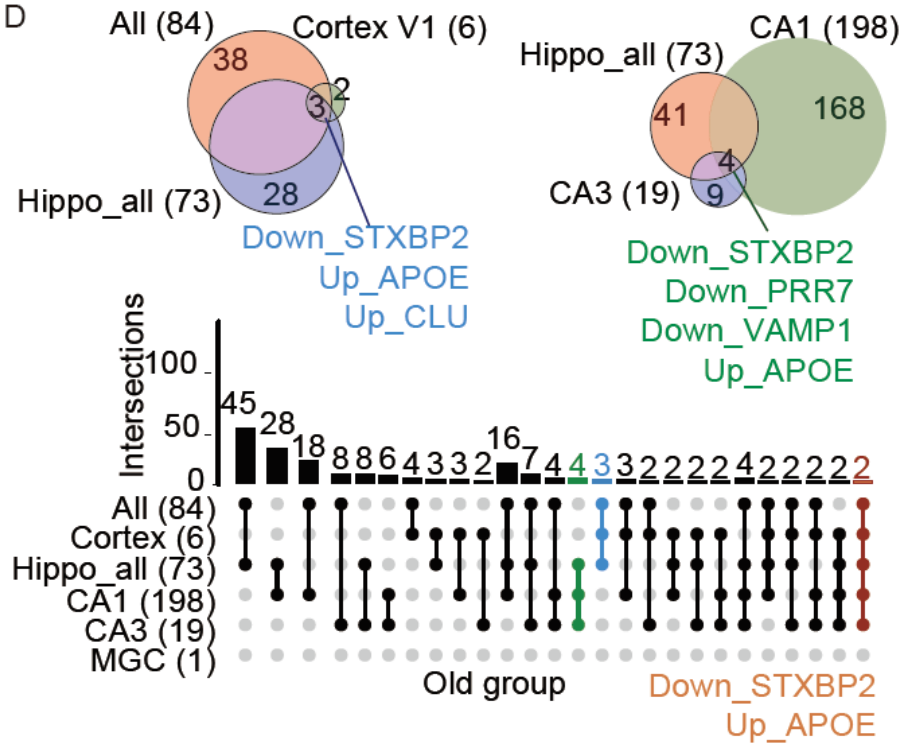

(B) t-SNE plot showing the sample clusters based on the prototype (n=3 mice per group). (C) Number of differentially expressed proteins in mouse brain. (D) Venn and upset diagrams showing the DEP overlaps for selected regions.

Proteomic profiling of normal and pathogenic brain tissue with subregion precision

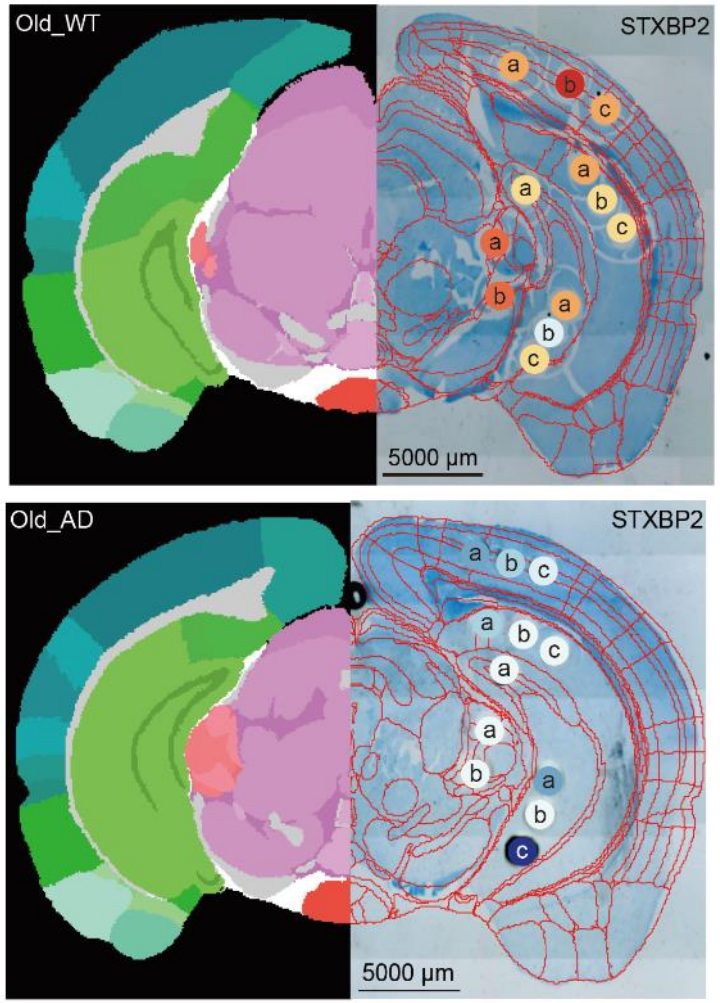

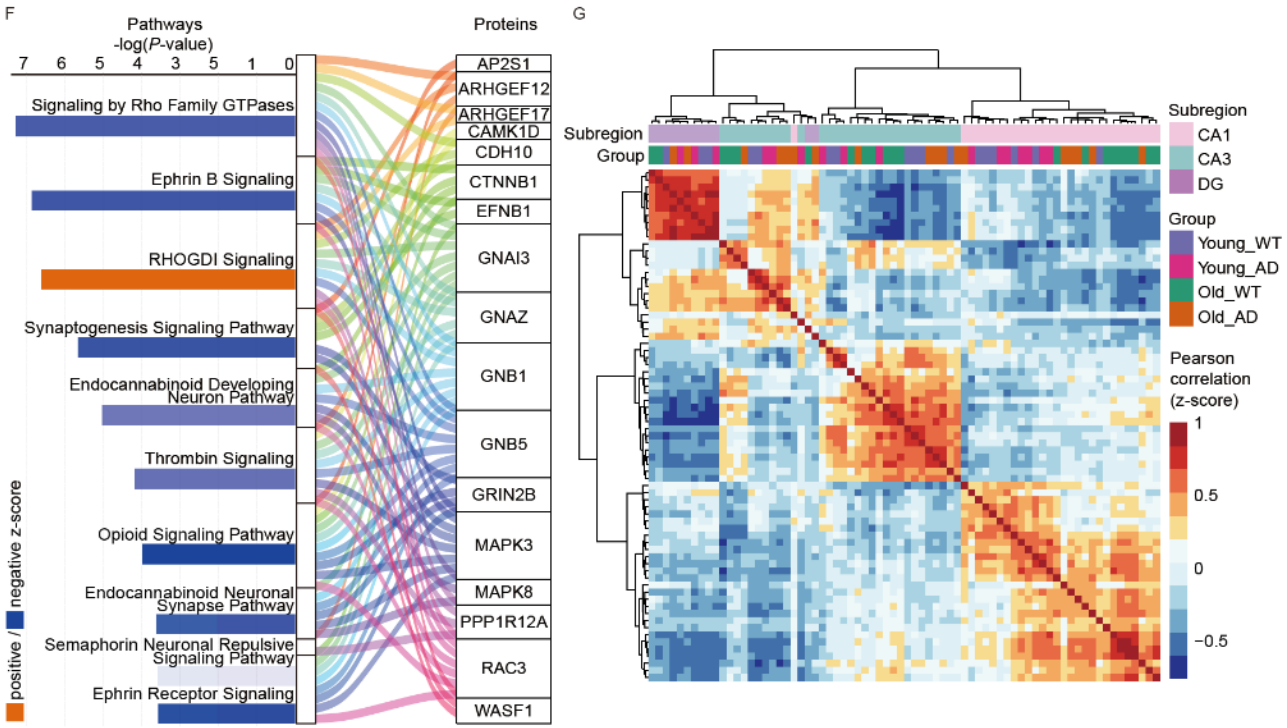

(E) Representative spatial proteomic maps of syntaxin binding protein 2 (STXBP2) in old WT and old AD brain slices. The a/b/c in the punches represents biological replicates from the same brain region. (F) Pathway enrichment of 198 DEPs in CA1 and Sanky plot exhibiting the correlation between enriched pathways and proteins. (G) The hierarchical clustering heatmap showing the z-score scaled Pearson correlation coefficients between two samples labeled by subregions of hippocampus and mouse group. The Pearson correlation coefficients were estimated by the abundance expression of 101 proteins.

ProteomEx: discussion and limitation

- ✓ We could achieve the lateral resolution of about 160 μm, which corresponds to ~262 cells or 0.61 nL tissue volume before expansion. The ProteomEx protocol is robust, cheap, easy to use, and can be readily deployed in a regular lab using commercially available reagents and common supplies.

- ✓ Enabling the handling of submillimeter gel pieces, for example, by employing robotics or microfluidics, can further improve the spatial resolution of ProteomEx.

- ✓ Since ProteomEx resembles protein-retention expansion microscopy, it can be combined with super-resolution microscopy of cellular structures and DNA and RNA fluorescence in situ hybridization enabling a spatially resolved multi-omics approach.

Acknowledgements

- We thank Rujie Qi and Yuan Yao from Westlake University for help with characterization of hydrogel mechanical stability. We also thank Xun Guo from Westlake University for help with tissue sample preparation.

THANK YOU

西湖大學
WESTLAKE UNIVERSITY